Pluronic-lysozyme conjugates as anti-adhesive and antibacterial bifunctional polymers for surface coating

Muszanska, Agnieszka K.; Busscher, Henk J.; Herrmann, Andreas; van der Mei, Henny C.; Norde, Willem

Published in:
Biomaterials

DOI:
10.1016/j.biomaterials.2011.05.016

Biomaterials 32 (2011) 6333–6341

Contents lists available at ScienceDirect

Biomaterials

journal homepage: www.elsevier.com/locate/biomaterials

Pluronic–lysozyme conjugates as anti-adhesive and antibacterial bifunctional polymers for surface coating

Agnieszka K. Muszanska [a], Henk J. Busscher [a], Andreas Herrmann [b], Henny C. van der Mei [a,*], Willem Norde [a,c]

[a] Department of Biomedical Engineering, W. J. Kolff Institute, FB40, University Medical Center Groningen and University of Groningen, P.O. Box 196, 9700 AD Groningen, The Netherlands
[b] Zernike Institute for Advanced Materials, University of Groningen, Nijenborgh 4, 9747 AG Groningen, The Netherlands
[c] Laboratory of Physical Chemistry and Colloid Science, Wageningen University and Research Center, P.O. Box 8038, 6700 EK Wageningen, The Netherlands

A R T I C L E I N F O

Article history:
Received 9 March 2011
Accepted 5 May 2011
Available online 28 May 2011

Keywords:
Block copolymers
Protein–polymer conjugates
Functional coatings
Medical applications

A B S T R A C T

This paper describes the preparation and characterization of polymer–protein conjugates composed of a synthetic triblock copolymer with a central polypropylene oxide (PPO) block and two terminal polyethylene oxide (PEO) segments, Pluronic F-127, and the antibacterial enzyme lysozyme attached to the telechelic groups of the PEO chains. Covalent conjugation of lysozyme proceeded via reductive amination of aldehyde functionalized PEO blocks (CHO-Pluronic) and the amine groups of the lysine residues in the protein. SDS-PAGE gel electrophoresis together with MALDI-TOF mass spectrometry analysis revealed formation of conjugates of one or two lysozyme molecules per Pluronic polymer chain. The conjugated lysozyme showed antibacterial activity towards *Bacillus subtilis*. Analysis with a quartz crystal microbalance with dissipation revealed that Pluronic–lysozyme conjugates adsorb in a brush conformation on a hydrophobic gold-coated quartz surface. X-ray photoelectron spectroscopy indicated surface coverage of 32% by lysozyme when adsorbed from a mixture of unconjugated Pluronic and Pluronic–lysozyme conjugate (ratio 99:1) and of 47% after adsorption of 100% Pluronic–lysozyme conjugates. Thus, bifunctional brushes were created, possessing both anti-adhesive activity due to the polymer brush, combined with the antibacterial activity of lysozyme. The coating having a lower degree of lysozyme coverage proved to be more bactericidal.

1. Introduction

Biomaterials in the human body are prone to bacterial infections, which may lead to the formation of a biofilm. Biofilm formation is preceded by protein adsorption, deposition of cells and bacteria. The complex structure of a biofilm, containing slime and extracellular polymeric matrix, makes it resistant to the host immune system as well as to antibiotic treatment [1]. Infection of implanted biomaterials usually requires secondary surgery [2,3]. Various biomaterials surface modifications have been developed to improve their antibacterial properties of implant surfaces, such as applying bactericidal agents [4], a hydrogel coating releasing bioactive antibodies [5], nitric oxide releasing substrates [6], a coating with furanones [7], chalcones [8], or various polymers [9]. Especially the later polymer brush coatings, have been proven in the past to reduce bacterial adhesion by one or two orders of magnitude [10–12], which makes them a promising tool for biomedical applications. A polymer brush is formed when highly soluble polymer chains are grafted to the surface at high packing density, forcing the polymer chains to extend into the surrounding aqueous medium. Thus, a highly hydrated polymer layer is formed at the surface, which acts as a barrier preventing deposition of particles, including bacteria [10]. Polymer chains can be grafted to the surface by simple physi-sorption, or by covalent bond formation. Chemical attachment makes the brush more stable but it is a complex and time-consuming procedure [13]. The grafting density plays a crucial role in the conformation of the adsorbed polymer layer. At low grafting densities, the polymer chains are coiled resulting in a so-called mushroom conformation of the adsorbed polymer molecule. At higher grafting densities, when the separation between the anchoring points is less than the hydrodynamic radius of the polymer coils, the polymer chains are forced to stretch into the surrounding medium forming a brush conformation [14]. In aqueous media, polyethylene oxide (PEO) is most often used as the soluble polymer. Ethylene oxide (EO) moieties

* Corresponding author. Tel.: +31503633140; fax: +31503633159.
E-mail address: h.c.van.der.mei@med.umcg.nl (H.C. van der Mei).

0142-9612/$ – see front matter © 2011 Elsevier Ltd. All rights reserved.
doi:10.1016/j.biomaterials.2011.05.016

in the PEO chain have a good structural fit with water molecules enabling a strong hydrogen bond between the ether oxygen of PEO and the hydrogen of water. Thus the PEO brush coating is highly hydrated. Compression of the PEO chains in the brush increases the osmotic pressure along with a reduction of their conformational entropy. This creates a strong repulsive force against deposition of indwelling particles, including bacteria [13,15,16].

The aim of this study is to design a bifunctional polymer brush coating by conjugation of an antibacterial compound with the polymer molecules so that the brush attains bi-functionality i.e., resistance to particle deposition and selective lethal interaction with microorganisms. For our study, we chose Pluronic F-127 as the PEO-containing polymer. Pluronics are a family of synthetic non-toxic neutral triblock copolymers made up of a central hydrophobic polypropylene oxide (PPO) block that is connected to two hydrophilic PEO side blocks, PEO_n–PPO_m–PEO_n. In aqueous medium this triblock copolymer self-assembles into micelles. After exposure to a hydrophobic surface, the micelles disaggregate in favour of adsorption. It is inferred that the hydrophobic PPO block attaches spontaneously to the surface, whereas the two PEO segments extend into the water phase [17,18]. Lysozyme was chosen as the antimicrobial agent because of its well known bactericidal properties [19,20], physiological abundance, high thermal stability with respect to structure [21], wide pH activity range [22], and well known structure [23,24]. Lysozyme is able to destruct bacterial cell walls by an enzymatic hydrolysis of 1,4-beta-linkages between N-acetylmuramic acid and N-acetyl-D-glucosamine residues of peptidoglycan in the bacterial cell wall, especially for Gram-positive bacteria [20]. Broadly directed activity makes lysozyme an important antimicrobial agent that can be used to prevent biomaterial associated infections by a wide variety of bacterial strains [25]. The use of polymer–protein conjugates is relatively new in biomedical research and has potential applications in drug delivery systems [26–28], and as novel biocompatible materials for e.g., implants and tissue engineering [29–32]. We used the protein–polymer conjugation approach [26] to synthesize lysozyme functionalized Pluronic molecules.

For lysozyme to exert enzymatic activity, it is desired, if not required, that it is exposed to the solution rather than being adsorbed to the surface. If the conjugate would adsorb with the lysozyme attached to the surface, the lysozyme would barely be accessible for the bacteria due to shielding by the polymer. Moreover, it has been reported that after adsorption on hydrophobic surfaces lysozyme looses its antimicrobial activity [33]. This implies that the conjugate should adsorb in a similar conformation as the unmodified Pluronic, i.e., via attachment of its PPO block, as shown in Fig. 1. Surface coatings consisting of Pluronic–lysozyme conjugates were characterized in terms of thickness, viscoelastic properties, surface composition and their anti-adhesive and antibacterial properties.

2. Materials and methods

2.1. Aldehyde-end functionalization of Pluronic F-127

5 M excess of Dess-Martin periodinane (1,1,1-tris(acetyloxy)-1,1-dihydro-1,2-benziodoxol-3(1H)-one, 97%, Sigma Aldrich, Germany) was added to a solution of 200 mg of Pluronic F-127 (PEO_{99}–PPO_{65}–PEO_{99}), MW = 12.6 kDa (BASF, Sigma Aldrich, Germany) in 20 ml of dry dichloromethane (Sigma Aldrich, Germany) at room temperature and stirred overnight. Thereafter, the reaction mixture was treated with cold diethyl ether ~30 ml (Merck, Germany). The precipitated product was cooled on an ice-water bath for 1 h, filtered off, washed with cold diethyl ether (2 × 20 ml) and dried under vacuum. The product was characterized by proton NMR in order to confirm conversion of the PEO hydroxy end-groups into aldehyde functionalities and the degree of conversion was determined using the Purpald colorimetric assay [34]. First, a calibration curve was recorded, in order to convert measured UV–VIS absorbance into number of aldehyde groups, using formaldehyde (37 wt% in H_2O, Sigma Aldrich, Germany), as described elsewhere [34]. Aldehyde functionalized Pluronic was dissolved in ultrapure water in a known range of concentrations. Next, 100 μl of polymer solution was added to 100 μl of 30 mM Purpald (4-amino-3-hydrazino-5-mercapto-1,2,4-triazole, Sigma Aldrich, Germany) solution in 2 M NaOH. After 15 min equilibration, 100 μl of a 30 mM sodium periodate ($NaIO_4$, Sigma Aldrich, Germany) solution in 0.2 M NaOH was added and oxidation

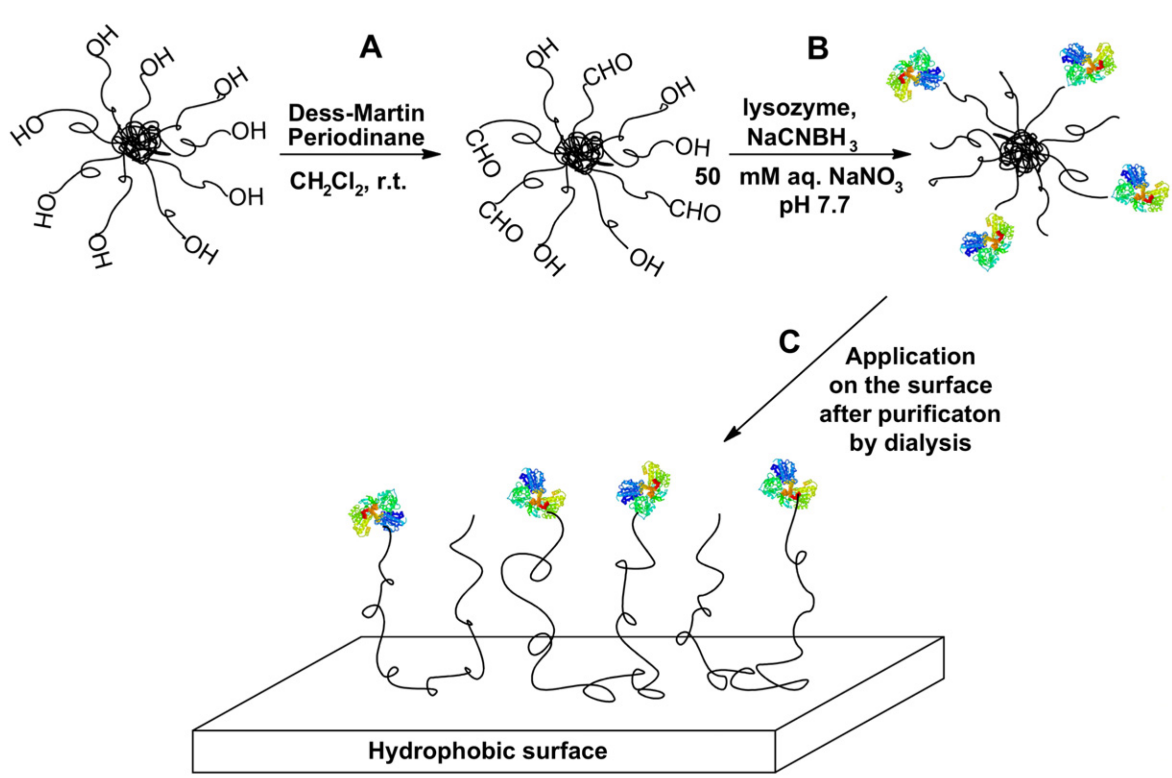

Fig. 1. Reaction scheme for the oxidation of Pluronic (A) and conjugation with lysozyme (B) forming micelles in aqueous medium, and adsorption on a hydrophobic surface into the brush conformation (C).

took place giving the mixture a purple colour. Changes in absorbance at 550 nm were measured by UV–VIS spectrophotometry.

2.2. Lysozyme conjugation

Lysozyme from chicken egg white (MW = 14.3 kDa, protein content ≥ 90%; Sigma Aldrich, Germany), was dissolved in 50 mM sodium nitrate ($NaNO_3$, Fluka, Germany) at pH 7.7, filtered over 0.22 μm pore size Acrodisc filter, to remove dust and minor impurities, and added dropwise to a stirred solution of aldehyde functionalized Pluronic (200 mg in 50 ml 50 mM $NaNO_3$ solution) at room temperature. After 20 min, 20 mg of sodium cyanoborohydride ($NaCNBH_3$, 95%; Sigma Aldrich, Germany) was added and the mixture was left stirring overnight at room temperature and pH 7.7. The molar ratio of lysozyme relative to aldehyde groups was chosen such that there was 10% molar excess of polymer aldehyde groups to amine groups from lysines in the lysozyme. Conjugation of protein to polymer was confirmed by sodium dodecyl sulphate polyacrylamide gel electrophoresis(SDS-PAGE) using NuPAGE Novex 4–12% Bis-Tris Gel (Molecular Probes, Invitrogen) stained with SimplyBlue™ safe stain (Molecular Probes, Invitrogen, The Netherlands). Then, the reaction mixture was placed into a dialysis tube (MWCO 25 kDa) and dialyzed against 50 mM sodium nitrate ($NaNO_3$, Fluka, Germany) at pH 7.7 for 5 days changing the surrounding medium every 24 h in order to remove unreacted protein together with free polymer molecules. The purification process was monitored by SDS-PAGE and when no more free lysozyme molecules were detected, the reaction mixture was freeze-dried and kept at −20 °C. Molecular weight of obtained conjugates was determined using a Voyager-DE Pro (Applied biosystems, USA) MALDI-TOF mass spectrometer. Samples were prepared by plate spotting of tested compounds, mixed with a sinapinic acid matrix. Pure lysozyme was used as a reference sample.

2.3. Enzymatic activity assay

The enzymatic activity of Pluronic–lysozyme conjugates was determined and compared with that of free lysozyme using *Bacillus subtilis* 168. *B. subtilis* was selected to evaluate the applicability of Pluronic–lysozyme conjugates as an anti-bacterial surface coating, as a representative of the many strains sensitive to lysozyme, including strains involved in biomaterial associated infections. Lysozyme destructs the bacterial cell wall by catalyzing hydrolysis of 1,4-beta-linkages between N-acetylmuramic acid and N-acetyl-D-glucosamine residues of peptidoglycan in the bacterial cell membrane. As a result, the turbidity of the bacterial suspension decreases, which can be followed spectrophotometrically by measuring the change in absorbance. Bacteria were first grown aerobically overnight at 37 °C on blood agar plate from frozen stock. Plates were kept at 4 °C and used no longer than for 2 weeks. One colony was used to inoculate 10 ml tryptone soya broth (TSB, OXOID, England). The pre-culture was incubated at 37 °C for 24 h and used to inoculate another culture of 200 ml TSB that was incubated for 16 h. The culture was harvested by centrifugation for 5 min at 5000×*g* and washed twice with phosphate buffered saline solution (PBS buffer, 10 mM potassium phosphate, 150 mM NaCl, pH 6.8). To break up aggregates bacteria were sonicated whilst cooling on an ice-water bath for 3 × 10 s at 30 W (Vibra Cell model 375; Sonics and Materials, USA). Finally, the bacteria were suspended in PBS buffer to an optical density at 600 nm (OD_{600}) of 0.500. For each enzymatic test, 1 ml of bacteria stock (OD_{600} = 0.500) was mixed with 100 μl of Pluronic–lysozyme conjugate of concentration 1 mg/ml or with free lysozyme at concentrations 0.05, 0.01, 0.005 mg/ml. Pluronic and PBS were used as control samples. Pure PBS buffer was used as a blank sample to calibrate the spectrophotometer. All measurements were done in triplicates at room temperature.

2.4. Quartz crystal microbalance with dissipation (QCM-D) measurements

Hydrated thickness and viscoelastic properties of adsorbed layers of unmodified Pluronic molecules, lysozyme conjugated Pluronic molecules and pure lysozyme molecules were studied using a QCM-D device, model Q-sense E4 (Q-sense, Sweden). Gold plated AT-cut quartz crystals, with a sensitivity constant of 17.7 ng/cm^2, were used as substratum. QCM-D has a distinctive advantage of elucidating interactions at a molecular level, by measuring the changes in frequency (*f*) and dissipation (*D*) of the gold crystal at 5 MHz oscillating frequency [35]. Prior to use, the gold surface of the crystals was cleaned by sonication in 2% SDS solution for 3 min, rinsed with ultrapure water, dried under a flow of filtered nitrogen gas and treated in an UV/ozone chamber for 10 min. These crystals were immersed in a heated (70 °C) mixture of ultrapure water, ammonia and hydrogen peroxide in a ratio 9:3:2 for 10 min. Next, they were rinsed with ultrapure water, again dried under a flow of filtered nitrogen gas and treated in a UV/ozone chamber for 10 min. The gold-coated quartz crystals were stored overnight in PBS buffer, yielding a hydrophobic gold surface with a water contact angle of 85 ± 1°. Crystal stability with respect to changes in the base lines for *f* and *D* during the flow of PBS adhesion buffer was monitored. After crystal stability was established, solutions of pure CHO-Pluronic, pure lysozyme, and Pluronic–lysozyme conjugate were flown separately on different gold surfaces in the QCM chamber at a flow rate of 24 s^{-1} at 25 °C and for 30 min. In a second set of experiments, CHO-Pluronic solution was flown over the 30 min old adsorbed pure lysozyme as well as pure lysozyme over the 30 min old adsorbed CHO-Pluronic in order to establish possible exchange between the two compounds at the surface. In a third set of experiments, the ratio of the Pluronic conjugated to lysozyme to unconjugated Pluronic, in the solution supplied to the surface, was varied (75%, 50%, 25%, 20%, 10%, 5%, 1%) and the corresponding solution was flown separately over the gold surface. All above-mentioned solutions were prepared in a concentration of 1 mg/ml of PBS adhesion buffer. At the end of each flow, all loosely adhered molecules were removed by rinsing with buffer.

During flow, changes in the frequency (*f*) and dissipation (D) were recorded and fitted using the Kelvin-Voight model, consisting of a spring and a dashpot assembly, at all overtones (3, 5, 7, 9 and 11) to evaluate the viscoelastic properties and the hydrated thickness of the adsorbed layer. The viscoelasticity was assessed in terms of relaxation time (τ), taken as a ratio of viscosity (η) and shear modulus (G). Viscosity and shear modulus of the adsorbed layers were calculated using software package Q-Tools 3.0.6, assuming that, in view of the low polymer fraction, the density of the adsorbed layer is 1000 kg/m^3. The viscosity of all solutions was measured and did not show a significant deviation from the viscosity of water, i.e. 1 m Pa s, which was used for all the calculations.

2.5. X-ray photoelectron spectroscopy measurements

Brushes on the gold plated crystal surfaces (see the above section) were subjected to surface chemical analysis, using X-ray photoelectron spectroscopy (XPS). Elemental compositions were measured using an S probe spectrophotometer (Surface Science Instruments, Mountain View, CA, USA) with X-rays (10 kV, 22 mA, spot size of 250 × 1000 μm) sourced from an aluminum anode with the analyzer placed at 35° take-off angle. The binding energy of broad spectrum survey scans was in the range of 1–1100 eV recorded at low resolution (pass energy 150 eV). Peaks over 20 eV binding energy range were recorded at high resolution (pass energy 50 eV) for C_{1s}, O_{1s}, N_{1s} and Au_{4f}. The area under each peak was used to calculate peak intensities after correction using the sensitivity factor provided by the manufacturer. N_{1s} electron counts from a densely packed crystalline lysozyme filled trough were assumed to correspond with 100% surface coverage by proteins and used to estimate the lysozyme surface coverage for each sample.

2.6. Adhesion and growth of bacteria in a parallel plate flow chamber

Bacterial suspensions were prepared as described above for the enzymatic activity assay. For each experiment, 200 ml suspension in PBS buffer was prepared at a concentration of 3 × 10^8 cells/ml. Implant grade silicone rubber sheets (thickness 0.5 mm, water contact angle 110 ± 1°, Medin, Groningen, The Netherlands) were used as substrata. Prior to use, they were cut into rectangular pieces (10 × 15 mm), rinsed with ethanol (97%, Merck, Darmstadt, Germany) and demineralised water. Next, they were sonicated for 3 min in 2% RBS 35 detergent (Omnilabo International BV, The Netherlands), subsequently rinsed with demineralised water, washed in methanol (Merck, Darmstadt, Germany) and again rinsed with demineralised water. The parallel plate flow chamber allows for a stable laminar flow with a shear stress τ and a shear rate σ, that can be calculated from the volumetric flow rate Q, according to:

$$\tau = \eta\sigma = \frac{\eta^3 Q}{2b^2 w} \tag{1}$$

where η is the absolute viscosity, and b and w are the flow chamber's depth and width, respectively [10]. Silicone rubber was fixed to the bottom plate of the chamber made of transparent thermoplastic poly(methyl methacrylate), whereas the top plate was made of glass. Before each experiment, the tubing and the chamber were filled with PBS buffer to remove air bubbles. Bottles containing bacterial suspension, buffer, polymer solution or bacterial medium were placed at a different height with respect to the chamber to create a hydrostatic pressure that allows the fluid to circulate through the chamber. Constant flow was maintained by recirculation, using a roller pump. A piece of silicone affixed at the bottom plate of the flow chamber was exposed for 30 min at room temperature to 1 mg/ml solutions of unconjugated Pluronic and Pluronic–lysozyme conjugates in varying ratios, i.e., 100%, and 1%, in separate sets of experiments. Non-attached molecules were removed by PBS buffer flow for 5 min. Then, the flow was switched from buffer to a bacterial suspension and bacteria were allowed to adhere for 2 h at room temperature under a shear stress of 0.005 Pa. Bacterial adhesion in PBS buffer was monitored real-time during the experiment using a fire wire CCD camera, mounted on the phase-contrast microscope and coupled to PC image analysis software. Each image was obtained from summation of 15 subsequent images with time intervals of 0.25 s to eliminate moving organisms from the analysis. From the images, numbers of bacteria adhering per unit area were determined as a function of time as a measure for the anti-adhesive functionality of the coatings.

Subsequently, unattached bacteria were flushed out by rinsing with PBS buffer for 5 min after which the flow was switched to 10% TSB medium to allow growth of adhering bacteria. The temperature was raised to 37 °C and the shear stress was decreased to 0.002 Pa for 20 h. Since the biofilm arising after growth of the adhering bacteria was too thick for enumeration of individual bacteria, 20 h old biofilms were removed from the substratum surfaces using a sterile cotton swab and suspended in 1 ml demineralised water. A dilution series of the bacterial suspension was plated on TSB agar to determine the absolute number of cultivable, live organisms (colony forming units or CFUs) on each surface. 10 μl of the suspension was transferred onto a glass slide and stained with live/dead stain (*Bac*LightTM, Molecular Probes Europe BV) to determine percentage viability of the bacteria using fluorescence microscopy (Leica, Wetzlar, Germany) as a measure for the antibacterial functionality of the coatings.

3. Results

3.1. Pluronic–lysozyme conjugation

The preparation of Pluronic–lysozyme conjugates is outlined in Fig. 1. The first step (A) involving Pluronic oxidation, was confirmed using Purpald colorimetric assay analysis, indicating 30% conversion of the hydroxyl end-groups (OH) into aldehyde functionalities (CHO). In the next step (B), the activated Pluronic molecules were coupled to lysine residues of lysozyme via reductive amination. Conjugate formation was confirmed by gel electrophoresis (Fig. 2A). Lane 1 shows the protein molecular weight marker, which is a mixture of purified proteins resolving in sharp bands from 10 to 140 kDa. This marker is used to compare the molecular weight of the obtained conjugates. Lane 2 in Fig. 2A shows Pluronic–lysozyme conjugates with molecular weights of 27 kDa and 41 kDa, respectively, and lane 3 represents free lysozyme. Since the average molecular weight of Pluronic F-127 is 12.6 kDa and that of lysozyme 14.3 kDa, a conjugate of one Pluronic molecule with one lysozyme molecule corresponds to MW 27 kDa and one Pluronic molecule coupled with two lysozyme molecules to MW 41 kDa. Moreover, lane 2 indicates the presence of remaining uncoupled lysozyme molecules, which were effectively removed by dialysis, as can be seen in lane 4. Molecular weights of the obtained conjugates were confirmed by MALDI-TOF mass spectrometry (see Fig. 2B). The mass spectrum of the purified sample shows characteristic peaks of the 1:1 Pluronic–lysozyme conjugate of MW 27 kDa (indicated as a in Fig. 2B) and the 1:2 Pluronic–lysozyme conjugate of MW 41 kDa (indicated as b in Fig. 2B). The strong peak to the left of 20 kDa peak, is expected to be a conjugate of one Pluronic with two lysozymes, appearing as a doubly charged molecular ion. Moreover, the mass spectrometric analysis confirms the effectiveness of the dialysis purification step since no free lysozyme molecules were detected.

3.2. Enzymatic activity assay of Pluronic–lysozyme conjugates

Data presented in Fig. 3 show that Pluronic–lysozyme conjugates of 1 mg/ml concentration exhibit similar antibacterial activity as free lysozyme in a concentration of 0.005 mg/ml. The optical density of bacterial suspensions of Pluronic–lysozyme conjugates (1 mg/ml) was reduced from 0.50 to 0.16 ± 0.01, whereas for free lysozyme (0.005 mg/ml) the reduction was from 0.50 to 0.18 ± 0.02. Furthermore, a decrease in optical density from 0.50 to 0.35 ± 0.02 and 0.37 ± 0.02 was observed for bacterial suspensions exposed to pure phosphate buffer saline (PBS) and uncoupled Pluronic (1 mg/ml), respectively.

3.3. Properties of adsorbed Pluronic–lysozyme conjugates

3.3.1. Quartz crystal microbalance with dissipation measurements

Fig. 4 shows the hydrated thickness (A) and relaxation time (B) upon exposure of the gold-coated quartz crystal to the various adsorbed compounds, i.e., (a) the uncoupled CHO-Pluronic, (b) lysozyme, (c) lysozyme after CHO-Pluronic, (d) CHO-Pluronic after lysozyme and (e) Pluronic–lysozyme conjugate 100%. The thickness of the 100% Pluronic–lysozyme conjugate is 14.3 ± 1.4 nm, which is greater than the sum of those calculated for CHO-Pluronic (5.8 ± 0.5 nm) and lysozyme (3.6 ± 0.5 nm). The relaxation time of the conjugate (7.9 ± 0.2) × 10^{-3} s does not significantly differ from that of the uncoupled CHO-Pluronic (7.5 ± 1.5) × 10^{-3} s, whereas it is much less than the relaxation time of adsorbed lysozyme (12.6 ± 2.9) × 10^{-3} s. Furthermore, both the thicknesses and relaxation times of lysozyme supplied to pre-adsorbed CHO-Pluronic (6.9 ± 0.4 nm and (8.5 ± 1.9) × 10^{-3} s, respectively) as well as CHO-Pluronic after lysozyme (5.8 ± 2.3 nm and (9.0 ± 1.5) × 10^{-3} s, respectively), resemble those recorded for exposure to only uncoupled CHO-Pluronic. Increasing the ratio of Pluronic conjugated with lysozyme to uncoupled Pluronic in the solution exposed to the surface, yields a change in the hydrated thickness from 7.1 ± 0.3 nm for 1% conjugation to 13.8 ± 0.5 nm for 25% conjugation, as presented in Fig. 5. Beyond a conjugation ratio of 25%, the hydrated thickness reached saturation. No significant changes in the

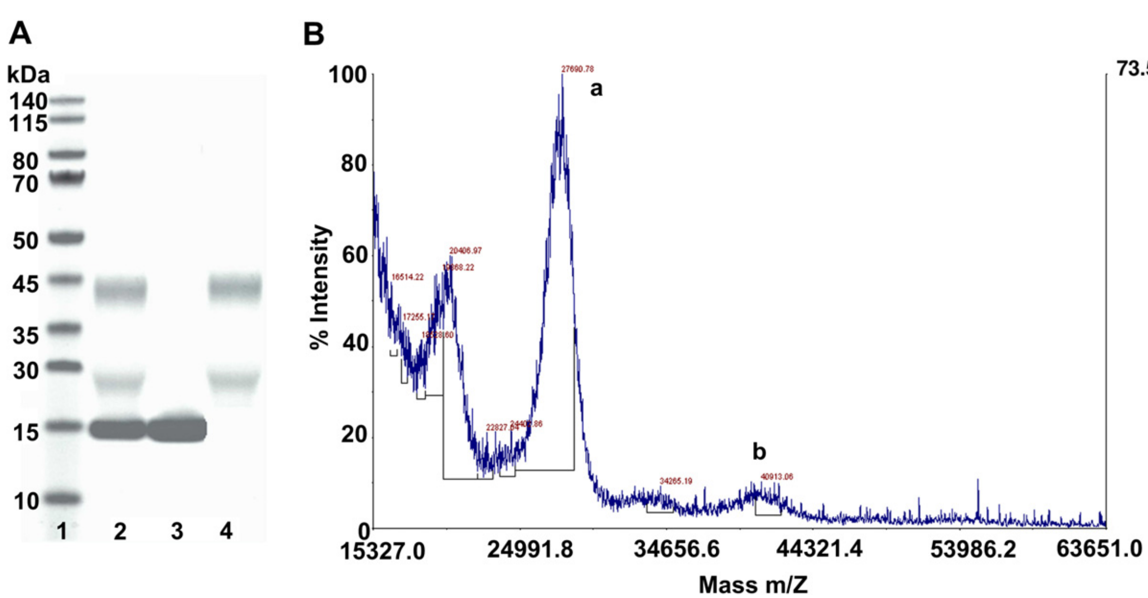

Fig. 2. (A) SDS-PAGE analysis, lane 1-molecular weight marker, lane 2– Pluronic coupled with lysozyme before purification (mixture of ∼27 kDa conjugates, ∼41 kDa conjugates and free lysozymes ∼14 kDa), lane 3 – free lysozyme, lane 4 – Pluronic coupled with lysozyme after dialysis (mixture of ∼27 kDa conjugates and ∼41 kDa conjugates).and (B) MALDI-TOF mass spectrum of Pluronic–lysozyme conjugates revealing successful coupling of one Pluronic molecule with one (a) and two lysozyme molecules (b).

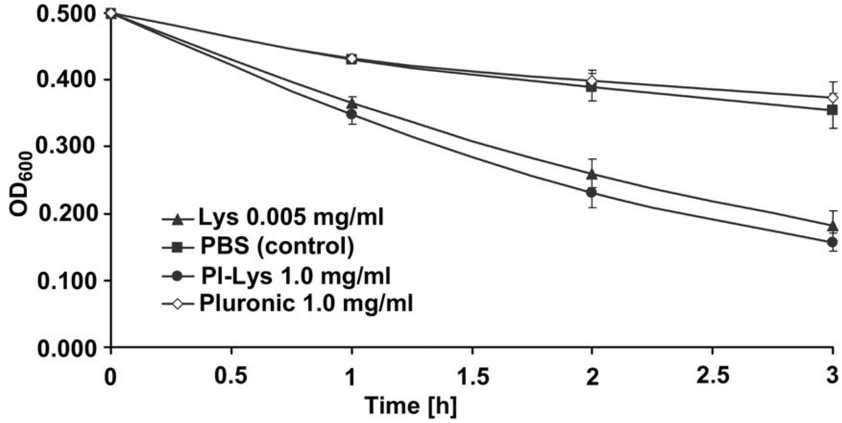

Fig. 3. Enzymatic activity of Pluronic–lysozyme (Pl-Lys) conjugates as a function of time, compared to the free lysozyme (Lys) activity, shown as a decrease in optical density OD_{600} of *B. subtilis* 168 caused by lysis of the bacterial cell wall. Error bars indicate standard deviation over three separate experiments.

relaxation time with different degree of conjugation were observed for either of the adsorbed compounds.

3.3.2. X-ray photoelectron spectroscopy measurements

Table 1 presents observed N_{1s} electron counts for each sample. Based on the number of counts, the gold-coated surface with only adsorbed lysozyme resulted in 50% protein coverage, whereas adsorption form a solution with 100% or 1% Pluronic–lysozyme conjugation yielded 47% and 32% coverage by lysozyme, respectively.

3.4. Bacterial adhesion and growth

Fig. 6 gives the number of adhering bacteria in the absence of growth on uncoated silicone rubber, on a coating of unmodified Pluronic and of Pluronic–lysozyme conjugates (1% and 100% conjugation ratios) as a function of time. Adhesion of *B. subtilis* 168 after 2 h was reduced from $(1.3 \pm 0.5) \times 10^5/cm^2$ on uncoated silicone rubber to $(0.2 \pm 0.1) \times 10^5/cm^2$ on an unconjugated Pluronic brush. Adhesion to 100% and 1% Pluronic–lysozyme conjugated brush coated surfaces resulted in $(1.1 \pm 0.2) \times 10^5$ and $(0.8 \pm 0.0) \times 10^5$ bacteria adhering per cm^2, respectively, attesting to their anti-adhesive functionality.

Fig. 7 shows that the total number of cultivable bacteria or CFUs present on the surfaces after 20 h growth is highest after coating with unconjugated Pluronic molecules, followed by uncoated silicone rubber. The number of CFUs present on a surface coated with a 100% Pluronic–lysozyme conjugate is reduced to about 30% and to 15% for 1% Pluronic–lysozyme conjugate, as compared with a coating consisting of unconjugated Pluronic molecules. After 20 h of growth, however, there are both cultivable, live bacteria as well as dead bacteria, as presumably killed by the coating, present. The fraction of live bacteria (see Fig. 7) on the uncoated silicone rubber is 69% and even 91% on unmodified Pluronic brush. However, in case of the lysozyme containing conjugates, the viability drops to 28% and 19% for coatings with 100% and 1% Pluronic–lysozyme conjugates, respectively. These finding attest to the antibacterial functionality, in addition to an anti-adhesive functionality.

4. Discussion

Anti-adhesive properties of polymer brush coatings have been reported in literature before [10,36], but interactions between bacteria and functionalized brushes have not received much attention so far. In this study, we present an approach for bioconjugate formation using a synthetic polymer, i.e. Pluronic and the protein lysozyme, in a two-step reaction. The resulting conjugates were characterized by SDS-PAGE gel electrophoresis, MALDI-TOF mass spectrometry and enzymatic activity assay. Physicochemical properties of surfaces coated with Pluronic–lysozyme conjugates were determined using QCM-D and XPS techniques. Anti-adhesive and antibacterial functionalities of the modified coatings were determined against *B. subtilis* in a parallel plate flow chamber in terms of the number of initially adhering bacteria per unit area and the number of viable bacteria after growth for 20 h.

4.1. Preparation and activity of Pluronic–lysozyme conjugates

The conjugation reaction of lysozyme molecules to the Pluronic F-127 polymer requires only a simple procedure, is reproducible, and cost effective without the need of substrate recovery. Therefore,

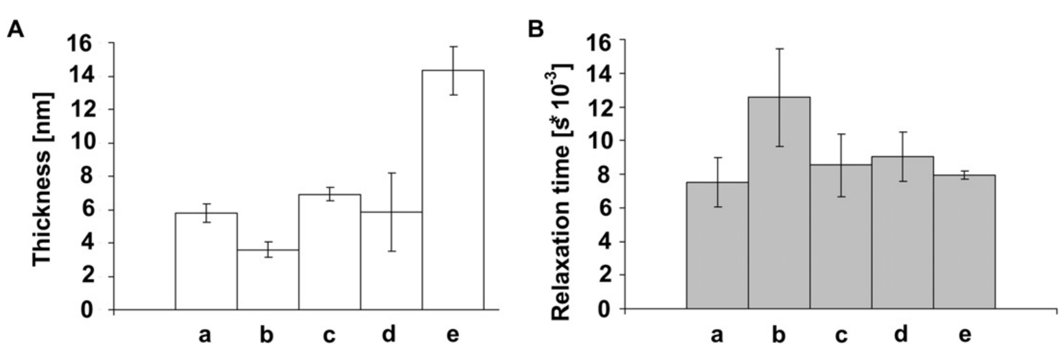

Fig. 4. Hydrated thickness (A) and relaxation time (B) determined by QCM-D of the adsorbed layers of (a) CHO-Pluronic, (b) lysozyme, (c) lysozyme after CHO-Pluronic, (d) CHO-Pluronic after lysozyme, (e) Pluronic–lysozyme conjugate 100%. Error bars indicate standard deviation over three separate experiments.

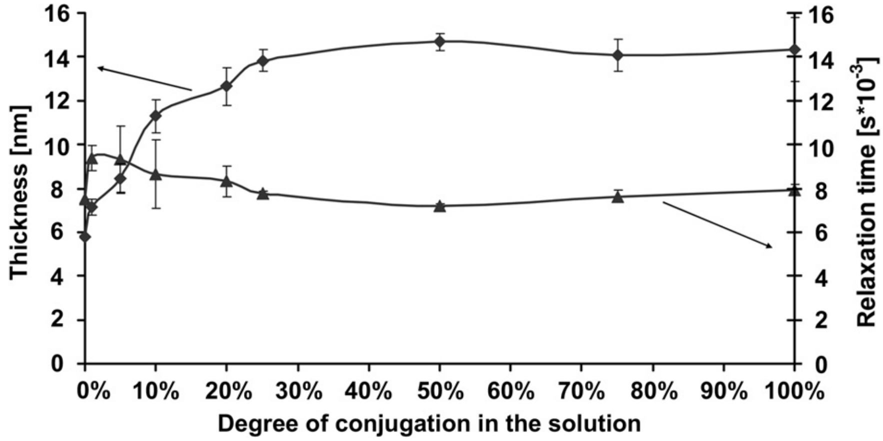

Fig. 5. Hydrated thickness and relaxation time of adsorbed layers of Pluronic–lysozyme conjugates as a function of the degree of conjugation (100% corresponds to one Pluronic chain coupled to one or two lysozyme molecules). Error bars indicate standard deviation over three separate experiments.

the coupling strategy involving two steps, i.e. alcohol oxidation followed by protein attachment by reductive amination, can be applied for other peptides and proteins as well. However, with lysozyme there is a risk of multi-conjugate formation because each lysozyme molecule contains six lysine residues, which gives the possibility of multiple couplings. Such a hybrid, where lysozyme is completely surrounded by polymer chains would be rather inactive due to reduced accessibility to the bacterial cell wall. To suppress the formation of multi-conjugates, the pH of the reaction mixture should be well controlled and maintained at ~7.7. For pH < 7 protonation of the $-NH_2$ groups of all six lysine residues makes the coupling reaction impossible to proceed and for pH > 8 all $-NH_2$ groups are deprotonated and, hence, available for coupling with the PEO blocks. Analysis of obtained conjugates shows the absence of multi-conjugates. SDS-PAGE together with mass spectrometry clearly showed the presence of conjugates composed of Pluronic molecules with one and two lysozymes per chain. The compound with a MW 20 kDa, which was detected by MALDI-TOF, but not by SDS-PAGE, is expected to be a conjugate of one Pluronic with two lysozymes, appearing as a doubly charged molecular ion. MALDI-TOF is a soft ionization method where the singly protonated molecular ions are usually the dominant species. However, they can be accompanied by doubly charged species at approximately half the m/Z value [37], which explains in our case the presence of a peak with half the MW of 41 kDa. The partial loss of lysozyme activity after coupling to the polymer chain may be caused by conformational changes in the protein structure and/or reduction in the enzyme–substrate contact.

Based on the molecular weights of both Pluronic and lysozyme, we estimate how much protein is present in 1 mg conjugate. Having a mixture of Pluronic coupled with one and Pluronic coupled with two lysozymes in an assumed ratio 1:1, we calculate that 1 mg contains 0.4 mg of Pluronic and 0.6 mg of lysozyme. This indicates activity loss of the conjugated proteins by a factor of 120 compared to free lysozyme. Although, this is a severe loss, the adhesion and growth data together with biofilm viability displayed in the Figs. 6 and 7, prove strongly remaining lysozyme activity in the conjugates when applied as a surface coating.

Table 1
N_{1s} electron counts of a lysozyme filled trough taken as a reference for 100% surface coverage by lysozyme and N_{1s} electron counts and surface coverages by lysozyme calculated for lysozyme on a gold surface and Pluronic–lysozyme (Pl–Lys) conjugates with different degrees of conjugation on silicone rubber.

Sample	N_{1s} counts	Surface coverage by lysozyme [%]
Trough filled with lysozyme (reference)	4268	100
Lysozyme deposited on gold	2110	50
100% Pl–Lys	2017	47
1% Pl–Lys	1349	32

4.2. Conformation of Pluronic–lysozyme conjugates at a hydrophobic surface

Pluronic molecules adsorb at a hydrophobic surface by attachment of their hydrophobic PPO block, whereas their PEO chains protrude in the aqueous solution [17]. Pluronic F-127 adsorption is dictated by the hydrophobicity of the substrate surfaces and adsorbs on different hydrophobic surfaces in the same conformation and with comparable thickness [39]. Hence, the structural information on the coating derived from QCM-D experiments using hydrophobic gold substrates may be correlated to the bacterial adhesion and viability tests performed in the parallel plate flow chamber on a hydrophobic silicone rubber biomaterial. After attachment of lysozyme to the terminal ends of the PEO chains, the adsorption behaviour of the conjugate may deviate from that of unmodified Pluronic. Lysozyme also has a tendency to adsorb to hydrophobic surfaces [38], and hence it may compete with the PPO block to attach to the surface. Obviously, the adsorbed Pluronic–lysozyme conjugate can adopt a brush or a pancake conformation (see Fig. 8a and b), depending on the adsorption affinity of lysozyme, relative to that of PPO, and on the loss of conformational entropy of the conjugate when it attaches via lysozyme at its terminal ends. It may also be possible that the conjugate anchors to the surface by both its PPO and lysozyme moieties as shown in Fig. 8c. The conformation of the layer of Pluronic–lysozyme conjugates on the surface was investigated by comparing values of their thickness and relaxation time with those of uncoupled lysozyme and Pluronic, obtained using QCM-D. The thickness of the uncoupled CHO-Pluronic (5.8 ± 0.5 nm) is in agreement with the thickness of a Pluronic brush of the same type [39]. The thickness of adsorbed lysozyme (3.6 ± 0.5 nm) corresponds to a monolayer with side-on adsorbed unperturbed lysozyme molecules having dimensions of 3.0 nm × 3.0 nm × 4.5 nm [22]. The thickness of the Pluronic–lysozyme conjugate is larger than the sum of those of CHO-Pluronic and lysozyme, suggesting that the lysozyme coupling forces the Pluronic to stretch out further into the solution. The observation that beyond a Pluronic–lysozyme : CHO-Pluronic ratio of 25% in solution, the thickness of the coating does not increase any further suggests preferential adsorption of the

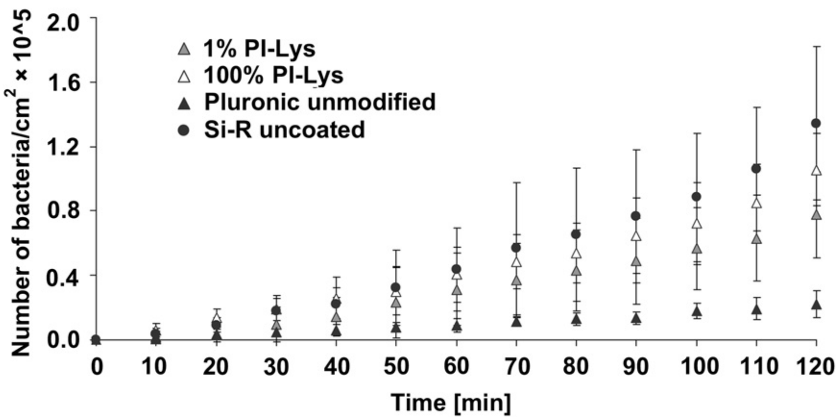

Fig. 6. Initial adhesion of *B. subtilis* 168 to uncoated (Si-R uncoated) and coated silicone rubber when adsorbed from a mixture of uncoupled Pluronic and Pluronic–lysozyme conjugate in 99:1 ratio (1% Pl–Lys) and 100% Pluronic–lysozyme conjugates (100% Pl–Lys) as a function of time. Error bars indicate standard deviation over four separate experiments.

Pluronic–lysozyme conjugate. The relaxation time of this conjugate resembles that of CHO-Pluronic rather than that of lysozyme, showing that the polymer part and not the protein part determines the viscoelastic properties. Adsorption of lysozyme after pre-adsorption of CHO-Pluronic, as well as sequential adsorption in the reversed order, yields values for thickness and relaxation time resembling those obtained for CHO-Pluronic and deviating from the values obtained for lysozyme. These observations provide strong evidence that in sequential adsorption, CHO-Pluronic does displace lysozyme from the surface, but that lysozyme is not able to displace adsorbed CHO-Pluronic. Apparently, the affinity of Pluronic for the hydrophobic gold surface is much higher than the affinity of lysozyme for that surface. From those data, we infer that the conjugate adsorbs by attaching its PPO block to the surface and the PEO chains with the attached lysozyme molecules are exposed to the solution. The strong attachment of the PPO block to the hydrophobic surface is in line with the high stability of Pluronic layers adsorbed at such a surfaces [40,41].

The occurrence of the adsorbed Pluronic–lysozyme conjugates in a brush-like conformation is further supported by the results from the bacterial adhesion and growth experiments, although adhesion of *B. subtilis* 168 is higher on a functionalized brush than on an unconjugated Pluronic brush coating, which might be ascribed to favourable electrostatic interaction between the positively charged lysozyme molecules and the negatively charged bacteria. This on its turn, is supported by the observation of an increased fraction of dead bacteria in the biofilm grown on coatings with Pluronic–lysozyme conjugated brushes.

4.3. Composition of the coating with respect to anti-adhesive and antibacterial functionalities

Varying the ratio between Pluronic–lysozyme conjugates and unmodified Pluronic in a brush, enables determination of the optimal composition of the coating. Results obtained by XPS analysis clearly show that the content of lysozyme in 100%

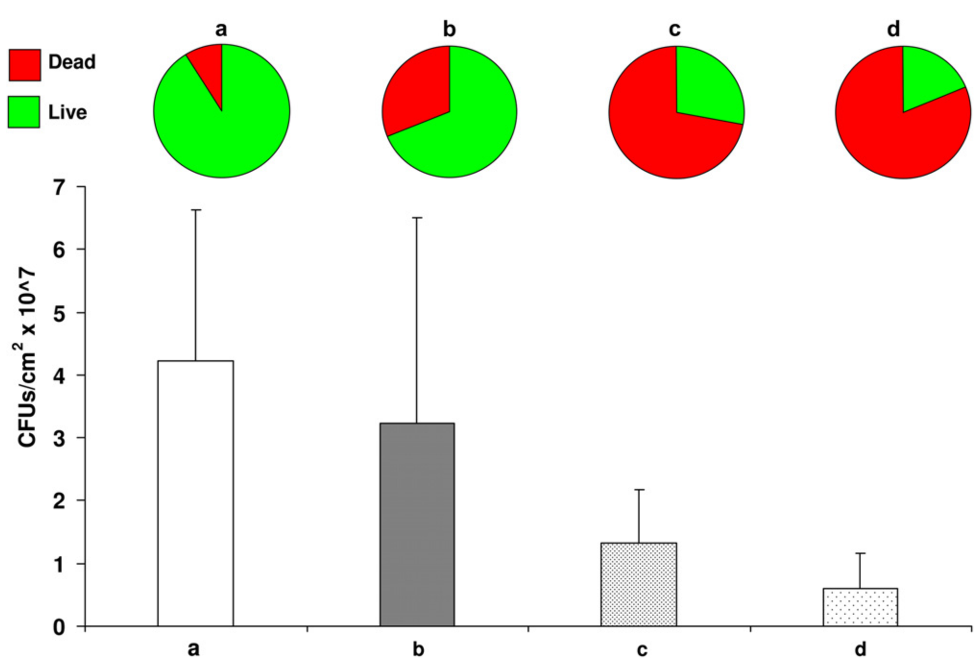

Fig. 7. CFUs per unit area of *B. subtilis* 168 after 20 h of growth on (a) Pluronic unmodified coating (b) uncoated silicone rubber (c) 100% Pluronic–lysozyme and (d) 1% Pluronic–lysozyme coated silicone rubber together with the percentage viability of the biofilms, represented by the pancakes. Error bars indicate standard deviation over four separate experiments. Live/dead percentage of bacteria represented by the pancakes include an average standard deviation of 5% over four separate experiments.

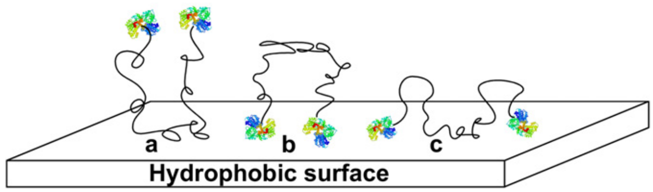

Fig. 8. Possible conformations of Pluronic–lysozyme conjugates adsorbed as (a) a brush with the Pluronic with its PPO block attached to the surface and the PEO chains with the lysozyme in the solution (b) a pancake with lysozyme adsorbed on the surface or (c) a structure where both lysozyme and the PPO of the Pluronic attach to the surface.

Pluronic–lysozyme conjugated coating is almost the same as when the surface is coated only with uncoupled lysozyme, corresponding to 47% surface coverage by lysozyme. Even for the coating formed after exposing the surface to a solution containing only 1% Pluronic–lysozyme conjugate, lysozyme coverage remains remarkably high, i.e., 32%. Again, this points to preferential adsorption of the conjugate relative to CHO-Pluronic. As expected, a lower surface coverage by lysozyme yields less bacterial adhesion, indicating that the anti-adhesive functionality of the Pluronic coating is preserved. The most viable biofilm was found on the unconjugated Pluronic brush coating, in line with previous work [10], in which it was found that bacteria growing on Pluronic brush coatings were less thick than on uncoated silicone rubber allowing more nutrients to penetrate into the adhering biofilm, yielding more viable bacteria. In fact, these observations prompted us to design a Pluronic brush coating with conjugated lysozyme, to reduce the viability of the few bacteria that managed to adhere and grow on a Pluronic brush coating. This requires an optimal amount of lysozyme in these coatings based on the preservation of anti-adhesive versus the development of bactericidal properties. However, and unexpectedly, the coating with the lower surface coverage by lysozyme is more effective in killing (i.e. causing lysing in this particular case) the bacteria than the brush prepared of a 100% Pluronic–lysozyme conjugate. One might wonder whether the efficacy of the surface coating changes when the surface first comes in contact with a protein-containing solution, such as most biofluids are (*e.g.* blood or saliva). If proteins would adsorb on the coated surface, this would most likely influence bacterial adhesion and/or viability. However, Norde and Gage [42] showed that a very similar Pluronic, $(PEO)_{100}$–$(PPO)_{56}$–$(PEO)_{100}$, exposed to a hydrophobic surface adopts a brush conformation having a sufficiently high density to strongly suppress protein adsorption. Hence, anti-adhesive and antibacterial functions of our coating are not expected to be lost after exposure to a protein-containing biofluid.

5. Conclusions

We presented a successful approach for preparing bioconjugates of synthetic polymers with natural proteins to be applied as functional coatings. Thus, brush coatings consisting of Pluronic and Pluronic–lysozyme conjugates were applied that exert bi-functionality, i.e. an anti-adhesive activity due to the polymer brush together with the antibacterial activity of the lysozyme. The work described in this paper contributes to a better understanding of the behaviour and surface properties of functionalized polymers, which may help to future development of more complex multi-functional coatings for application in biological systems, including coating of biomaterials implant surfaces.

Funding

This research was funded by the University of Groningen-University Medical Center Groningen, Groningen, The Netherlands.

Referrences

[1] Gristina AG. Implant failure and the immune-incompetent fibro-inflammatory zone. Clin Orthop Relat Res 1994;298:106–18.
[2] Gristina AG. Biomaterial-centered infection – microbial adhesion versus tissue integration. Science 1987;237:1588–95.
[3] Stickler DJ, Mclean RJC. Biomaterials associated infections – the scale of the problem. Cell Mater 1995;5:167–82.
[4] Zhao LZ, Chu PK, Zhang YM, Wu ZF. Antibacterial coatings on titanium implants. J Biomed Mater Res B 2009;91:470–80.
[5] Rojas IA, Slunt JB, Grainger DW. Polyurethane coatings release bioactive antibodies to reduce bacterial adhesion. J Control Release 2000;63:175–89.
[6] Charville GW, Hetrick EM, Geer CB, Schoenfisch MH. Reduced bacterial adhesion to fibrinogen-coated substrates via nitric oxide release. Biomaterials 2008;29:4039–44.
[7] Baveja JK, Wilcox MDP, Hume EBH, Kumar N, Odell R, Poole-Warren LA. Furanones as potential anti-bacterial coatings on biomaterials. Biomaterials 2004;25:5003–12.
[8] Sivakumar PM, Iyer G, Natesan L, Doble M. 3'-Hydroxy-4-methoxychalcone as a potential antibacterial coating on polymeric biomaterials. Appl Surf Sci 2010;256:6018–24.
[9] Leckband D, Sheth S, Halperin A. Grafted poly(ethylene oxide) brushes as nonfouling surface coatings. J Biomater Sci Polym Ed 1999;10:1125–47.
[10] Nejadnik MR, Van der Mei HC, Norde W, Busscher HJ. Bacterial adhesion and growth on a polymer brush-coating. Biomaterials 2008;29:4117–21.
[11] Raynor JE, Capadona JR, Collard DM, Petrie TA, Garcia AJ. Polymer brushes and self-assembled monolayers: versatile platforms to control cell adhesion to biomaterials. Biointerphases 2009;4:FA3–16.
[12] Ayres N. Polymer brushes: applications in biomaterials and nanotechnology. Polym Chem 2010;1:769–77.
[13] Currie EPK, Norde W, Stuart MAC. Tethered polymer chains: surface chemistry and their impact on colloidal and surface properties. Adv Colloid Interface Sci 2003;100:205–65.
[14] Sofia SJ, Premnath V, Merrill EW. Poly(ethylene oxide) grafted to silicon surfaces: grafting density and protein adsorption. Macromolecules 1998;31:5059–70.
[15] FreijLarsson C, Nylander T, Jannasch P, Wesslen B. Adsorption behaviour of amphiphilic polymers at hydrophobic surfaces: effects on protein adsorption. Biomaterials 1996;17:2199–207.
[16] Alexandridis P, Hatton TA. Poly(ethylene oxide)-poly(propylene oxide)-poly(ethylene oxide) block-copolymer surfactants in aqueous-solutions and at interfaces – thermodynamics, structure, dynamics, and modeling. Colloids Surf A Physicochem Eng Asp 1995;96:1–46.
[17] Schroen CGPH, Stuart MAC, Maarschalk KV, Van der Padt A, Van't Riet K. Influence of preadsorbed block-copolymers on protein adsorption – surface properties, layer thickness, and surface coverage. Langmuir 1995;11:3068–74.
[18] Otsuka H, Nagasaki Y, Kataoka K. Self-assembly of poly(ethylene glycol)-based block copolymers for biomedical applications. Curr Opin Colloid Interface Sci 2001;6:3–10.
[19] Masschalck B, Michiels CW. Antimicrobial properties of lysozyme in relation to foodborne vegetative bacteria. Crit Rev Microbiol 2003;29:191–214.
[20] Arnheim N, Inouye M, Law L, Laudin A. Chemical studies on enzymatic specificity of goose egg-white lysozyme. J Biol Chem 1973;248:233–6.
[21] Czeslik C, Winter R. Effect of temperature on the conformation of lysozyme adsorbed to silica particles. Phys Chem Chem Phys 2001;3:235–9.
[22] Vertegel AA, Siegel RW, Dordick JS. Silica nanoparticle size influences the structure and enzymatic activity of adsorbed lysozyme. Langmuir 2004;20:6800–7.
[23] Prager EM, Arnheim N, Wilson AC, Mross GA. Amino-acid sequence studies on bobwhite quail egg-white lysozyme. J Biol Chem 1972;247:2905–16.
[24] Strynadka NCJ, James MNG. Lysozyme revisited – crystallographic evidence for distortion of an N-acetylmuramic acid residue bound in site-D. J Mol Biol 1991;220:401–24.
[25] Yuan S, Wan D, Liang B, Pehkonen SO, Ting YP, Neoh KG, et al. Lysozyme-coupled poly(poly(ethylene glycol)) methacrylate-stainless steel hybrids and their antifouling and antibacterial surfaces. Langmuir 2011;27:2761–74.
[26] Danial M, Klok HA, Norde W, Stuart MAC. Complex coacervate core micelles with a lysozyme-modified corona. Langmuir 2007;23:8003–9.
[27] Tao L, Liu JQ, Xu JT, Davis TP. Synthesis and bioactivity of poly(HPMA)-lysozyme conjugates: the use of novel thiazolidine-2-thione coupling chemistry. Org Biomol Chem 2009;7:3481–5.
[28] Yi X, Batrakova E, Banks WA, Vinogradov S, Kabanov AV. Protein conjugation with amphiphilic block copolymers for enhanced cellular delivery. Bioconjug Chem 2008;19:1071–7.
[29] Chung HJ, Go DH, Bae JW, Jung IK, Lee JW, Park KD. Synthesis and characterization of Pluronic((R)) grafted chitosan copolymer as a novel injectable biomaterial. Curr Appl Phys 2005;5:485–8.
[30] Thordarson P, Le Droumaguet B, Velonia K. Well-defined protein-polymer conjugates-synthesis and potential applications. Appl Microbiol Biotechnol 2006;73:243–54.
[31] Shachaf Y, Gonen-Wadmany M, Seliktar D. The biocompatibility of pluronic (R) F127 fibrinogen-based hydrogels. Biomaterials 2010;31:2836–47.
[32] Gonen-Wadmany M, Oss-Ronen L, Seliktar D. Protein–polymer conjugates for forming photopolymerizable biomimetic hydrogels for tissue engineering. Biomaterials 2007;28:3876–86.

[33] Schmidt CF, Zimmermann RM, Gaub HE. Multilayer adsorption of lysozyme on a hydrophobic substrate. Biophys J 1990;57:577–88.
[34] Quesenberry MS, Lee YC. A rapid formaldehyde assay using purpald reagent: application under periodation conditions. Anal Biochem 1996;234:50–5.
[35] Voinova MV, Rodahl M, Jonson M, Kasemo B. Viscoelastic acoustic response of layered polymer films at fluid-solid interfaces: continuum mechanics approach. Phys Scr 1999;59:391–6.
[36] Brittain WJ, Minko S. A structural definition of polymer brushes. J Polym Sci A Polym Chem 2007;45:3505–12.
[37] Gross JH. Mass spectrometry. A textbook. Springer-Verlag; 2005. pp. 507–560.
[38] Wertz CF, Santore MM. Adsorption and reorientation kinetics of lysozyme on hydrophobic surfaces. Langmuir 2002;18:1190–9.
[39] Nejadnik MR, Olsson ALJ, Sharma PK, Van der Mei HC, Norde W, Busscher HJ. Adsorption of Pluronic F-127 on surfaces with different hydrophobicities probed by quartz crystal microbalance with dissipation. Langmuir 2009;25:6245–9.
[40] Liu X, Wu D, Turgman-Cohen S, Genzer J, Theyson TW, Rojas OJ. Adsorption of a nonionic symmetric triblock copolymer on surfaces with different hydrophobicity. Langmuir 2010;26:9565–74.
[41] Hellmich W, Regtmeier J, Duong TT, Ros R, Anselmetti D, Ros A. Poly(oxyethylene) based surface coatings for poly(dimethylsiloxane) microchannels. Langmuir 2005;21:7551–7.
[42] Norde W, Gage D. Interaction of bovine serum albumin and human blood plasma with PEO-tethered surfaces: influence of PEO chain length, grafting density and temperature. Langmuir 2004;20:4162–7.